Coulomb Excitation of ⁸⁰Sr and the limits of the $N \approx Z \approx 40$ island of deformation

R. Russell, J. Heery, J. Henderson, R. Wadsworth, K. Kaneko, N. Shimizu, T. Mizusaki, Y. Sun, 6 C. Andreoiu, D. W. Annen, A. A. Avaa, G. C. Ball, V. Bildstein, S. Buck, C. Cousins, A. B. Garnsworthy, S. A. Gillespie, ¹⁰ B. Greaves, ⁹ A. Grimes, ⁸ G. Hackman, ⁸ R. O. Hughes, ¹¹ D. G. Jenkins, ² T. M. Kowalewski, ^{12,13} M. S. Martin, 14, † C. Müller-Gatermann, 15 J. R. Murias, 8 S. Murillo Morales, 8 S. Pascu, 1, 16 D. M. Rhodes, 8, 11 J. Smallcombe, ¹⁷ P. Spagnoletti, ⁷ C. E. Svensson, ^{8,9} B. Wallis, ² J. Williams, ⁸ C. Y. Wu, ¹¹ and D. Yates ^{8,18} ¹School of Maths and Physics, University of Surrey, Guildford, GU2 7XH, Surrey, United Kingdom ²School of Physics, Engineering and Technology, University of York, York, YO10 5DD, North Yorkshire, United Kingdom ³Department of Physics, Kyushu Sangyo University, Fukuoka 813-8503, Japan ⁴Center for Computational Sciences, University of Tsukuba, Tennodai, Tsukuba 305-8577, Japan ⁵Institute of Natural Sciences, Senshu University, Tokyo 101-8425, Japan ⁶School of Physics and Astronomy, Shanghai Jiao Tong University, Shanghai 200240, China ⁷Department of Chemistry, Simon Fraser University, Burnaby, V5A 1S6, British Columbia, Canada ⁸ TRIUMF, Vancouver, V6T 2A3, British Columbia, Canada ⁹Department of Physics, University of Guelph, Guelph, N1G 2W1, Ontario, Canada ¹⁰Facility for Rare Isotope Beams, Michigan State University, East Lansing, 48824, Michigan, USA ¹Lawrence Livermore National Laboratory, Livermore, 94550, California, USA ¹²Department of Physics and Astronomy, University of North Carolina, Chapel Hill, 27599, North Carolina, USA ¹³ Triangle Universities Nuclear Laboratory, Duke University, Durham, 27708, North Carolina, USA ¹⁴Department of Physics, Simon Fraser University, Burnaby, V5A 1S6, British Columbia, Canada ¹⁵Physics Division, Argonne National Laboratory, Lemont, 60439, Illinois, USA ¹⁶National Institute for Physics and Nuclear Engineering, Bucharest-Magurele, R-77125, Romania ¹⁷ Japan Atomic Energy Agency, Naka-gun, 319-1184, Ibaraki, Japan ¹⁸Department of Physics and Astronomy, University of British Columbia, Vancouver, V6T 1Z4, British Columbia, Canada

The region of $N\approx Z\approx 40$ has long been associated with strongly deformed nuclear configurations. The presence of this strong deformation was recently confirmed through lifetime measurements in $N\approx Z$ Sr and Zr nuclei. Theoretically, however, these nuclei present a challenge due to the vast valence space required to incorporate all necessary orbitals. Recent state-of-the-art predictions indicate a near axial prolate deformation for N=Z and N=Z+2 nuclei between N=Z=36 and N=Z=40. In this work we investigate the shores of this island of deformation through a sub-barrier Coulomb excitation study of the N=Z+4 nucleus, 80 Sr. Extracting a spectroscopic quadrupole moment of $Q_s(2_1^+)=0.5_{-0.9}^{+0.8}$ eb, we find that 80 Sr is inconsistent with significant axial prolate deformation with a significance of 1.5σ . This result, albeit with a large uncertainty, indicates that the predicted region of strong prolate deformation around N=Z=40 is tightly constrained to the quartet of nuclei: 76,78 Sr and 78,80 Zr.

INTRODUCTION

The atomic nucleus exhibits a number of emergent properties arising from the underlying structure of its nucleons. Among these is collectivity, arising from the collective motion of nucleons as the nucleus deviates from sphericity, which is a key test of nuclear models, necessarily involving multiple nucleons within the nucleus. Quadrupole deformation in the upper fpg region of nuclei, delimited by the N = Z nuclei ⁵⁶Ni and ¹⁰⁰Sn, has long challenged configuration-interaction type nuclear models. This is due to the strong influence of the interaction between the $1g_{9/2}$ orbital below N=Z=50and the $2d_{5/2}$ orbital residing outside of the nominal fpg space, requiring a vast valence space to capture the necessary correlations. This effect is further exacerbated at the line of N=Z, where the protons and neutrons occupy the same single-particle orbitals and thus experience enhanced correlations due to their large spatial overlap.

The region around N=Z=38 ⁷⁶Sr and N=Z=40

 $^{80}\mathrm{Zr}$ has long been associated with strong deformation [1–3]. The extent of the quadrupole deformation in the region was recently verified through lifetime measurements [4] of the first 2^+ state in $^{80}\mathrm{Zr}$. This work also confirmed the enhanced deformation previously reported in $^{76}\mathrm{Sr}$ [5]. These measurements yield $B(E2)=120(^{+18}_{-14})$ W.u. and B(E2)=93(9) W.u. for $^{76}\mathrm{Sr}$ and $^{80}\mathrm{Zr}$, respectively, indicative of strongly deformed $(\beta_2\approx0.4)$ nuclear systems. Heavier isotopes of strontium, meanwhile, have also been found to be strongly collective, with B(E2)=93(5) W.u. in $^{78}\mathrm{Sr}$ (N=Z+2) and B(E2)=94(4) W.u. in $^{80}\mathrm{Sr}$ (N=Z+4), seemingly placing them within this region of strong deformation.

Recent developments in nuclear-structure theory have yielded promising results in this region [6], demonstrating the emergence of deformation at N=Z=40 using the the pairing-plus-multipole Hamiltonian with the monopole-based universal force (PMMU) [7, 8]. In Ref. [6], N=Z and N=Z+2 nuclei were investigated using the PMMU interaction, making use of both Monte-Carlo Shell Model (MCSN) and Hartree-

Fock Bogolyubov plus generator coordinate method (HFB+GCM) many body methods. Collective observables were extracted, with the authors highlighting the role of the quadrupole-quadrupole interaction between the $1g_{9/2}$ and $2d_{5/2}$ orbitals across the N=50 and Z=50 shell gaps. It was found that calculations incorporating the gd interaction predicted strongly deformed, prolate systems between N=Z=36 and N=Z=40. whereas the suppression of the gd QQ interaction entirely eliminated this effect, resulting in modestly deformed oblate systems. For more details of the PMMU interaction and the methods used, the reader is referred to Refs. [6–8]. Further to the strongly-deformed nature of the nuclei around $N \approx Z \approx 40$, we note that $^{80}{\rm Zr}$ has also been predicted to exhibit multiple shape coexistence, with five 0^+ states predicted below 2.25 MeV [9], highlighting the complex interplay between nuclear configurations in this region of the nuclear landscape.

In this work we clarify the nature of the nuclear shape approaching the region of strong deformation around $N \approx Z \approx 40$. For the first time we are able to employ a method sensitive to the underlying nuclear shape, presenting the first sub-barrier Coulomb excitation measurement of ⁸⁰Sr, lying only two protons and two neutrons "South East" of N = Z = 40 ⁸⁰Zr. In doing so we are able to access the spectroscopic quadrupole moment of the first 2^+ state, $Q_s(2_1^+)$. This is a key observable in understanding the collective properties of the nucleus, and can be related to the specific shape of the intrinsic nuclear deformation: prolate vs. oblate vs. triaxial. Therefore, we can constrain the limit of the predicted island of strong, axial, prolate deformation approaching $N \approx Z \approx 40$.

EXPERIMENTAL METHODS

The experiment was carried out at the TRIUMF-ISAC facility, with the use of the γ -ray detection array TI-GRESS [10, 11]. Radioactive ⁸⁰Sr was produced using the isotope-separation online (ISOL) method. The TRI-UMF cyclotron impinged a 520-MeV proton beam upon a thick niobium target, producing radioisotopes which were then extracted using the Ion-Guide Laser Ion Source (IG-LIS) [12]. IG-LIS suppresses surface-ionised products using a repeller electrode held at 40 V, permitting only neutral atoms to escape the target volume. After diffusing from the target volume, the strontium atoms are selectively ionized through resonant ionization and mass separated, providing a purified beam of ⁸⁰Sr. The singly-charged ions are then charge bred using the electron cyclotron resonance (ECR) charge state breeder (CSB) [13, 14], prior to injection into the ISAC and ISAC-II accelerator chain. The use of the CSB introduces stable contaminants into the beam, of which the most problematic for the present work are isobars of ⁸⁰Sr.

in particular 80 Se which dominated the beam composition (approximately 98.4% of the total, as determined with the TRIFIC ionization chamber [15]), and 80 Kr (approximately 1.3%), which was also produced in the decay of 80 Sr within the CSB. The beam was then accelerated to $4.25\,\mathrm{MeV/u}$ and delivered to the experimental station.

The beam was impinged upon a $0.882 \,\mathrm{mg/cm^2}$ target of ²⁰⁸Pb at the centre of TIGRESS, with S3-type annular silicon particle detectors located 27-mm upstream and 33-mm downstream of the target, as used in e.g. [16]. TI-GRESS was in its "forward" configuration, with the front suppressors partially withdrawn, allowing the HPGe detectors to be closely packed around the target chamber and in order to maximize detection efficiency. Excited states in the beam and target nuclei were populated through Coulomb excitation, with scattered nuclei detected in the S3 detectors. Prompt γ -rays from the de-excitation of the populated excited states were detected in TIGRESS. The data were analyzed using the GRSISort [17] analysis package built in the ROOT [18] framework. Scattered particles were selected and identified as A = 80 (beam-like) and A = 208 (target-like) on the basis of their kinematics, as shown in Fig. 1. Gammaray energies were added-back based on coincident hits in immediately neighboring HPGe crystals to maximize efficiency and suppress Compton background. Comptonscatters were further suppressed on the basis of hits in the TIGRESS Compton veto detectors. Gamma-ray energies were then corrected for their Doppler shift on the basis of the two-body scattering kinematics, yielding the γ -ray spectra shown in Fig. 2. Clearly, the spectra are dominated by the excitation of the strong ⁸⁰Se contaminant in the beam, with a $2^+_1 \rightarrow 0^+_1$ transition energy of 666 keV. The $2^+_1 \rightarrow 0^+_1$ transition in $^{80}{\rm Sr}$ was, however, visible above the Compton scattering background at 386 keV (see Fig.2), allowing for its yield as a function of scattering angle to be extracted. The peak area was extracted using a combined fit, obtained through a chi^2 minimization, with a Gaussian peak and a second-order polynomial background fitted to the experimental data for each angular range. Alternative background parameterizations were investigated but were not found to significantly impact the result, fluctuations between them were incorporated into the uncertainty on the yield as a function of scattering angle.

Yields from Coulomb excitation were evaluated using the semi-classical coupled channels Coulomb excitation code GOSIA [19], with the SRIM [20] software package employed to account for energy loss of ions in the target. An external χ^2 minimisation was used, in conjunction with GOSIA, which uses the ROOT MINUIT libraries [21]. The experimental data were divided into thirteen angular ranges, with six used for the detection of beam-like particles in the downstream detector, six for detection of target-like particles in the downstream detector, and a single angular range for detections in the

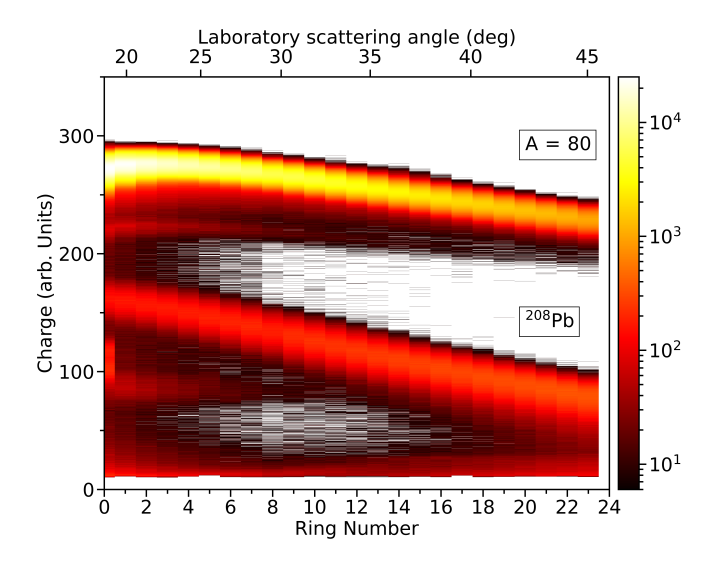


FIG. 1. Charge detected in the rings of the downstream S3 detector. The laboratory angles are shown on the upper axis. The top band are the A=80 nuclei, such as the desired $^{80}\mathrm{Sr},$ and the lower band are the $^{208}\mathrm{Pb}$ nuclei which have been scattered by the beam-like particles. Other smaller features in the data are attributed to A/Q contaminants in the beam, present at a lower level than the A=80 nuclei and excluded on the basis of kinematic selection. Note that, for the purpose of presentation, bins containing less than 5 counts have been omitted from this figure.

upstream detector, due to lower statistics at backwards angles. This provides for a near continuous coverage from approximately $30^{\circ} \rightarrow 160^{\circ}$ in the centre-of-mass frame. Due to the large ⁸⁰Se contamination, normalisation to a target transition was not possible and the minimisation therefore used the adopted literature value of B(E2; $2_1^+ \rightarrow 0_1^+) = 94(4)\,\mathrm{W.u.}$ in ⁸⁰Sr, as an additional constraint [22].

RESULTS

The dominant source of uncertainty in the present result arose from the large Compton background on which the 386-keV ⁸⁰Sr peak was located. Every effort was made to reduce this background, including the use of the Compton suppression shields mounted on the TI-GRESS array and the application of appropriate multiplicity gates to the experimental data. Even with these efforts, the uncertainty remained dominated by this background, to the extent that all other systematic contributions to the uncertainty are largely negligible. We emphasize, however, that the key experimental observable in determining the quadrupole moment reported here is the relative γ -ray yield as a function of scattering angle, and thus the contaminants within the beam are only relevant insofar as the background they induce in the spectrum. In spite of the dominance of the background in the un-

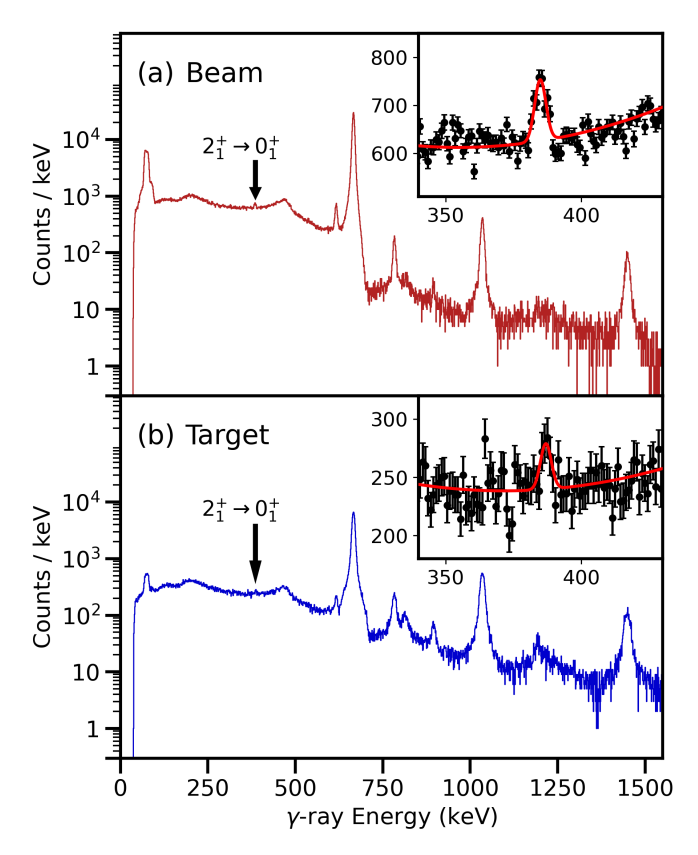


FIG. 2. (a) Addback γ-ray spectra with Compton suppression for detected A=80 nuclei over all rings of the Si detector, Doppler corrected for A=80 nuclei. (b) As (a) but for detected $^{208}{\rm Pb}$ nuclei with a Doppler correction for A=80 nuclei for Si detector rings 13-24, corresponding to centre-of-mass angles 90° - 110°. Insets: These show the 386 keV $2_1^+ \rightarrow 0_1^+$ transition for $^{80}{\rm Sr},$ with fits to the data as described in the text. The unmarked major peaks seen in this figure are from other A=80 beam-like projectiles, with the strongest peak at 666 keV corresponding to the decay of the 2_1^+ state in $^{80}{\rm Se}.$

certainty evaluation, we briefly discuss some systematic contributions below that were included within the analysis.

One key contribution to Coulomb excitation is the role of multi-step excitations. These excitations can result in interference terms due to the relative signs of the matrix elements involved. It was found that the impact of interference from the higher states on the 2_1^+ state was negligible. An additional consideration in this analysis was the low 0_2^+ state observed in Ref. [23] to be at 1000(100) keV. This level is expected to have an E2 transition to 2_1^+ and an E0 transition to 0_1^+ similar to those seen in work for other nuclei in this region [24, 25]. To ensure that there was no undue strength attributed to this $0_2^+ \to 2_1^+$ transition, an E0 transition will need to be accounted for in the analysis for which GOSIA has no facility at present. This leads to the method seen to be used in Refs. [26–28] where a pseudo 1^+ level is made

in GOSIA for the purpose of adding M1 de-excitations following the $0_2^+ \to 1_{pseudo}^+ \to 0_1^+$ path. It was found that there was no strong influence of this transition on the experimental results obtained here, with a systematic contribution to $Q_s(2_1^+)$ of 0.01 eb.

We note that two experimental values exist for the $B(E2;0_1^+\to 2_1^+)$ in the literature from Refs. [29] and [1]. In order to investigate the correlation between $Q_s(2_1^+)$ and $B(E2;0_1^+\to 2_1^+)$ value, and any influence from the choice of literature $B(E2;0_1^+\to 2_1^+)$ on the quoted $Q_s(2_1^+)$, we performed a χ^2 analysis for varying $\langle 0_1^+|E2|2_1^+\rangle$, as shown in Fig. 3 (a). Only a minimal correlation was found, with the χ^2 distribution corresponding to the $B(E2;0_1^+\to 2_1^+)$ from Ref. [29] shown in Fig. 3 (b). The effects of the correlation are included in the uncertainty quoted below.

With the above considerations and analysis, we obtain $Q_s(2_1^+) = 0.5_{-0.9}^{+0.8}$ eb in $^{80}\mathrm{Sr}$. While the present result has large uncertainty, it still excludes a large range of the available $Q_s(2_1^+)$ space permitted within the bounds of standard collective behavior. To demonstrate this, we consider $Q_s(2_1^+)/|Q_s^{rot}(2_1^+)|$, where

$$Q_s^{rot}(2_1^+) = \frac{2}{7} \sqrt{\frac{16\pi}{5} \cdot B(E2; 0_1^+ \to 2_1^+)}. \tag{1}$$

This ratio, also referred to in the literature as the reduced quadrupole moment (q_s) [30], can also be equated approximately to $-\cos(3\gamma)$ in the strongly-deformed regime [31]. The experimental value for $Q_s(2_1^+)$ yields $Q_s(2_1^+)/|Q_s^{rot}(2_1^+)| = 0.5(9)$, which is discrepant from the prolate limit $(Q_s(2_1^+)/|Q_s^{rot}(2_1^+)| = -1)$ with a significance of 1.5 σ . The distribution of the experimental yields compared to the extracted value and the axial prolate limit can be seen in Fig. 4.

We now compare this result to state-of-the art calculations performed using the method outlined in Ref. [6]. Here, the PMMU interaction is used with a large model space $(2p_{3/2}, f_{5/2}, 2p_{1/2}, 1g_{9/2}, 2d_{5/2})$. This model space has been shown to be essential in reproducing prolate deformation in N=Z nuclei beyond A=70, where the quadrupole-quadrupole qd interaction plays a dominant role in inducing nuclear deformation. Further to results for 76,78 Sr and other N=Z and N=Z+2 isotopes, presented in Ref. [6], we present here calculations for ⁸⁰Sr, summarized in Fig. 5 (a). The PMMU calculations predict a large, negative $Q_s(2_1^+)$ value, at approximately the prolate axial limit (i.e. $Q_s(2_1^+)/|Q_s^{rot}(2_1^+)| \approx -1$), in disagreement with the present experimental result. The calculations successfully reproduce the experimentally observed [22] B(E2; $2_1^+ \rightarrow 0_1^+$) = 94(4) W.u with B(E2; $2_1^+ \to 0_1^+)_{PMMU} = 96.5$ W.u, as well as the level energies for the 2_1^+ and 4_1^+ states. We note that the calculations of Ref. [6] predict a shape transition to occur between A = 80 and A = 84, along the line of N = Z, with prolate and oblate shape-minima near-degenerate

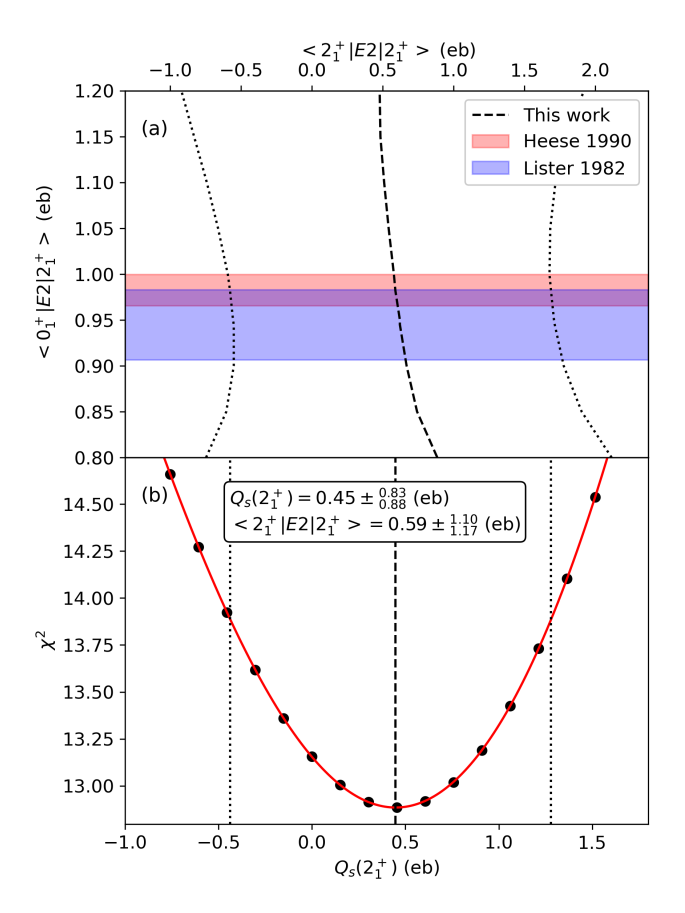


FIG. 3. (a) $Q_s(2_1^+)$ extracted in the present work, plotted against the $\langle 0_1^+|E2|2_1^+\rangle$ matrix element. The bottom axis is $Q_s(2_1^+)$ while the top axis is the corresponding matrix element $\langle 2_1^+|E2|2_1^+\rangle$. The quoted $Q_s(2_1^+)$ in this work uses the result from Heese 1990 [29] (red band), which is taken as the evaluated [22] value. The dashed line corresponds to the $Q_s(2_1^+)$ value with the minimum χ^2 for the given $\langle 0_1^+|E2|2_1^+\rangle$ value, while the dotted lines correspond to $\chi^2_{\min}+1$. The intersection of the present data with the second most precise result, taken from Ref. [1] (Lister 1982) is also shown, having only a very minor impact on the final extracted $Q_s(2_1^+)$ value. (b) The fitted χ^2 plotted as a function of $\langle 2_1^+|E2|2_1^+\rangle$ matrix element (top axis) and $Q_s(2_1^+)$ (bottom axis). Shown by the dashed line is the minimum value, while the dotted lines indicate the $\chi^2_{min}+1$ limits, yielding $Q_s(2_1^+)=0.5_{-0.9}^{+0.8}$ eb.

at ⁸⁴Mo. In addition, whereas PMMU shell model calculations predict a sudden transition from axial prolate to axial oblate deformation in Ref. [6], HFB+GCM calculations predict an intermediate nucleus: ⁸²Zr, in which $Q_s(2_1^+)/|Q_s^{rot}(2_1^+)|\approx -0.5$ lies between the two axial solutions. One might therefore hypothesize that ⁸⁰Sr could be a similar case, lying in a transitional region between axially prolate nuclei ^{76,78}Sr and ⁸⁰Zr, and axially oblate nuclei residing at and beyond ⁸⁴Mo.

To investigate further, we compare to level energy systematics. The ratio of the 4_1^+ and 2_1^+ energies (R_{42}) in particular is well-established as a metric by which to

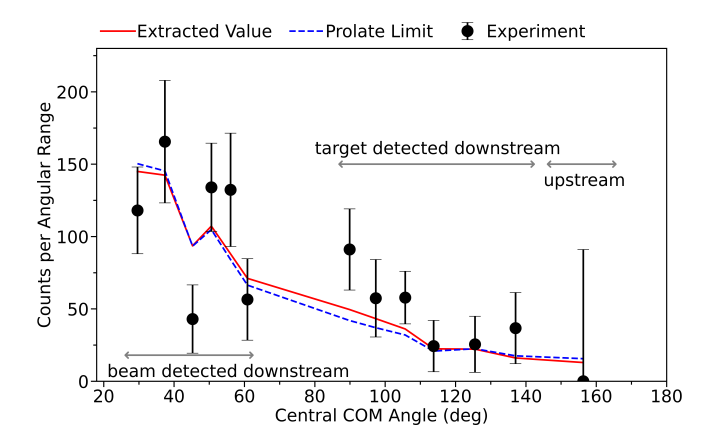


FIG. 4. The distribution of the experimental yields over their centre-of-mass angles. Compared to the experimentally measured data are the corresponding extracted values and those relating to the prolate limit. For the minimised value $\chi^2=12.8~(\chi^2_{\nu}=1.07)$, and for the prolate limit $\chi^2=15.0~(\chi^2_{\nu}=1.25)$, with 12 degrees of freedom.

distinguish rigid rotors ($R_{42} = 3.33$) from vibrational $(R_{42} = 2)$ systems. This ratio is plotted against neutron number for Kr, Sr and Zr isotopes in Fig. 5 (b) and for N = 40,42 isotones against proton number in Fig. 5 (c). Notably, no nuclei considered here reach the rotational limit, which can be explained by an enhancement in the ground-state binding due to proximity to the line of N=Z (see e.g. Ref. [32]). Nonetheless, $^{80}\mathrm{Sr}$ exhibits a consistently lower R_{42} value than 76,78 Sr and 80 Zr, for which R_{42} approaches a local maximum, and instead remains approximately consistent with its N=42isotonic partners. The even-even isotonic neighbor of ⁸⁰Sr, ⁷⁸Kr, has been investigated thoroughly through Coulomb excitation [33], permitting a full analysis using the Kumar-Cline rotational invariants [34, 35]. These invariants allow for a model independent determination of $\langle \cos(3\gamma) \rangle = 0.41(6)$, indicating a significant role for triaxiality in that system. The measured $Q_s(2_1^+)$ value in the present work is compatible with that expected for a similar level of triaxiality to that experimentally observed in $^{78}\mathrm{Kr}$.

CONCLUSIONS

To conclude, we report on a sub-barrier Coulomb excitation measurement of $^{80}\mathrm{Sr},$ performed at TRIUMF-ISAC. Despite large background present in this work, we are able to report the first measurement of $Q_s(2_1^+)=0.5_{-0.9}^{+0.8}$ in $^{80}\mathrm{Sr}.$ Comparison with the expected value for a rigid rotor indicates a system which has not reached prolate axiality, and behaves consistently with its N=42 isotonic neighbors. A comparison was performed with calculations performed with the PMMU interaction which are able to include interactions between the key

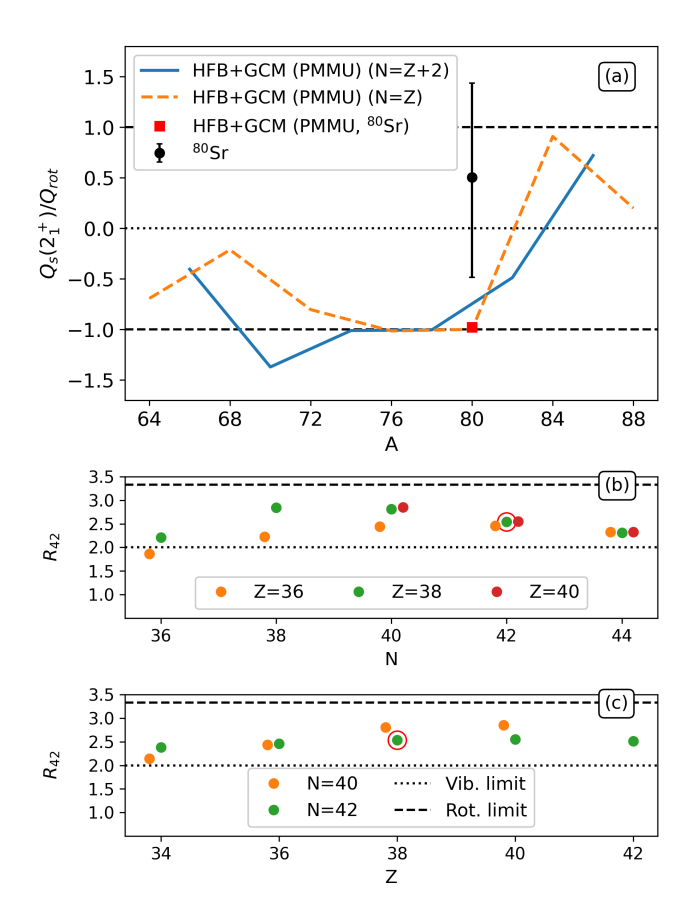


FIG. 5. (a) The ratio of the spectroscopic quadrupole moment $(Q_s(2_1^+))$ to the rotational limit (Q_{rot}) defined in Eq. 1, as calculated from Ref. [6] using the PMMU interaction with the Hartree-Fock Bogoliubov plus Generator Coordinate Method (HFB + GCM) method, showing N=Z and N=Z+2 values separately. Also shown is the experimental ratio deduced in the present work for 80 Sr, and the theoretical value for 80 Sr, calculated using the HFB + GCM method (red square). (b) The ratios of the 4_1^+ energy to the 2_1^+ energy (R_{42}) for Kr (Z=36), Sr (Z=38) and Zr (Z=40) isotopes as a function of neutron number, N. (c) R_{42} for N=40 and N=42 isotones, as a function of proton number, Z. Strontium-80 is highlighted in both (b) and (c) with a red circle. The vibrational and rotational R_{42} limits are indicated by the dotted and dashed lines, respectively.

 $1g_{9/2}2d_{5/2}$ orbitals, and which predict a $Q_s(2_1^+)$ value more consistent with an axially prolate system. These calculations, however, predict a shape change between the prolate and oblate minima to occur between $^{80}\mathrm{Zr}$ and $^{84}\mathrm{Mo}$, with N=42 $^{82}\mathrm{Zr}$ a transitional point. One hypothesis would be that $^{80}\mathrm{Sr}$ might similarly lie in this transitional region. Importantly, with the present result inconsistent with axial prolate deformation at the level of more than 1.5σ , it indicates that the anticipated island of strongly deformed axial systems around N=Z=40 is likely confined to $^{76,78}\mathrm{Sr}$ and $^{78,80}\mathrm{Zr}$. Further measurements to reduce the uncertainty on $Q_s(2_1^+)$ and to per-

form a more complete sum-rule analysis will be essential to completely delimit the region of deformation around N=Z=40, as well as measurements on more neutron-deficient isotopes of strontium and zirconium event closer to the line of N=Z.

ACKNOWLEDGEMENTS

The authors thank the beam-delivery team at TRIUMF-ISAC for providing the beams which were used in the present work. RR thanks J. Russell for useful discussions. Work at the University of Surrey was supported under UKRI Future Leaders Fellowship grant no. MR/T022264/1. Work at the University of Surrey and University of York was supported by the Science and Technologies Facilities Council (STFC) under grants ST/V001108/1 (Surrey), ST/P003885 (York) and ST/V001035 (York). This work has been supported by the Natural Sciences and Engineering Research Council of Canada (NSERC), The Canada Foundation for Innovation and the British Columbia Knowledge Development Fund. TRIUMF receives federal funding via a contribution agreement through the National Research Council of Canada. Supported by the U.S. Department of Energy, Office of Science, Office of Nuclear Physics under contract DE-AC02-06CH11357. Work at Lawrence Livermore National Laboratory was performed under the auspices of the U.S. Department of Energy under contract DE-AC52-07NA27344.

The data that support the findings of this article are not publicly available upon publication because it is not technically feasible and/or the cost of preparing, depositing, and hosting the data would be prohibitive within the terms of this research project. The data are available from the authors upon reasonable request.

- * jack.henderson@surrey.ac.uk
- [†] Present Address: Physics Division, Argonne National Laboratory, Lemont, 60439, Illinois, USA
- C. J. Lister, B. J. Varley, H. G. Price, J. W. Olness, Extreme Prolate Deformation in Light Strontium Isotopes, Phys. Rev. Lett. 49 (1982) 308–311.
- [2] C. J. Lister, M. Campbell, A. A. Chishti, W. Gelletly, L. Goettig, R. Moscrop, B. J. Varley, A. N. James, T. Morrison, H. G. Price, J. Simpson, K. Connel, O. Skeppstedt, Gamma radiation from the N=Z nucleus ⁸⁰/₄₀Zr₄₀, Phys. Rev. Lett. 59 (1987) 1270–1273.
- [3] R. Sahu, S. P. Pandya, Structure of the heaviest selfconjugate nucleus ⁸⁰Zr, Journal of Physics G: Nuclear Physics 14 (1988) L165.
- [4] R. D. O. Llewellyn, M. A. Bentley, R. Wadsworth, H. Iwasaki, J. Dobaczewski, G. de Angelis, J. Ash, D. Bazin, P. C. Bender, B. Cederwall, B. P. Crider, M. Doncel, R. Elder, B. Elman, A. Gade, M. Grinder,

- T. Haylett, D. G. Jenkins, I. Y. Lee, B. Longfellow, E. Lunderberg, T. Mijatović, S. A. Milne, D. Muir, A. Pastore, D. Rhodes, D. Weisshaar, Establishing the Maximum Collectivity in Highly Deformed N=Z Nuclei, Phys. Rev. Lett. 124 (2020) 152501.
- [5] A. Lemasson, H. Iwasaki, C. Morse, D. Bazin, T. Baugher, J. S. Berryman, A. Dewald, C. Fransen, A. Gade, S. McDaniel, A. Nichols, A. Ratkiewicz, S. Stroberg, P. Voss, R. Wadsworth, D. Weisshaar, K. Wimmer, R. Winkler, Observation of mutually enhanced collectivity in self-conjugate ⁷⁶₃₈sr₃₈, Phys. Rev. C 85 (2012) 041303.
- [6] K. Kaneko, N. Shimizu, T. Mizusaki, Y. Sun, Triple enhancement of quasi-SU(3) quadrupole collectivity in Strontium-Zirconium N≈Z isotopes, Physics Letters B 817 (2021) 136286.
- [7] K. Kaneko, T. Mizusaki, Y. Sun, S. Tazaki, Toward a unified realistic shell-model hamiltonian with the monopole-based universal force, Phys. Rev. C 89 (2014) 011302.
- [8] K. Kaneko, Y. Sun, G. de Angelis, Enhancement of high-spin collectivity in n=z nuclei by the isoscalar neutron-proton pairing, Nuclear Physics A 957 (2017) 144– 153.
- T. R. Rodríguez, J. L. Egido, Multiple shape coexistence in the nucleus ⁸⁰Zr, Physics Letters B 705 (2011) 255– 259.
- [10] G. Hackman, C. E. Svensson, The TRIUMF-ISAC gamma-ray escape suppressed specrometer, TIGRESS, Hyperfine Interactions 225 (2014) 241–251.
- [11] H. Scraggs, C. Pearson, G. Hackman, M. Smith, Austin. G. Ball, A. Boston, P. Bricault, Chakrawarthy. R. Churchman. N. Cowan. G. Cronkhite, E. Cunningham, T. Drake, P. Finlay, P. Garrett, G. Grinver, B. Hyland, B. Jones, J. Leslie, J.-P. Martin, D. Morris, A. Morton, A. Phillips. F. Sarazin, M. Schumaker, C. Svensson, J. Valiente-Dobón, J. Waddington, L. Watters, L. Zimmerman, TIGRESS highly-segmented high-purity germanium clover detector, Nuclear Instruments and Methods in Physics Research Section A: Accelerators, Spectrometers, Detectors and Associated Equipment 543 (2005) 431 - 440.
- [12] S. Raeder, H. Heggen, J. Lassen, F. Ames, D. Bishop, P. Bricault, P. Kunz, A. Mjøs, A. Teigelhöfer, An ion guide laser ion source for isobar-suppressed rare isotope beams, Review of Scientific Instruments 85 (2014) 033309.
- [13] K. Jayamanna, D. Yuan, M. Dombsky, P. Bricault, M. McDonald, M. Olivo, P. Schmor, G. Stanford, J. Vincent, A. Zyuzin, A design of an ECR ion source for radioactive ion beams for ISAC on-line facility at TRIUMF, Review of Scientific Instruments 73 (2002) 792–794.
- [14] F. Ames, K. Jayamanna, D. H. L. Yuan, M. Olivo, R. Baartman, P. Bricault, M. McDonald, P. Schmor, T. Lamy, Charge State Breeding with an ECRIS for ISAC at TRIUMF, AIP Conference Proceedings 749 (2005) 147–150.
- [15] A. Chester, J. Smallcombe, J. Henderson, J. Berean-Dutcher, N. Bernier, S. Bhattacharjee, A. Garnsworthy, S. Georges, S. Gillespie, G. Hackman, B. Olaizola, O. Paetkau, C. Pearson, B. Undseth, D. Yates, Trific: The triumf fast ion counter, Nuclear Instruments and Methods in Physics Research Section A: Accelerators, Spectrometers, Detectors and Associated Equipment 930

 $(2019)\ 1-7.$

- [16] S. A. Gillespie, J. Henderson, K. Abrahams, F. A. Ali, L. Atar, G. C. Ball, N. Bernier, S. S. Bhattcharjee, R. Caballero-Folch, M. Bowry, A. Chester, R. Coleman, T. Drake, E. Dunling, A. B. Garnsworthy, B. Greaves, G. F. Grinyer, G. Hackman, E. Kasanda, R. LaFleur, S. Masango, D. Muecher, C. Ngwetsheni, S. S. Ntshangase, B. Olaizola, J. N. Orce, T. Rockman, Y. Saito, L. Sexton, P. Šiurytė, J. Smallcombe, J. K. Smith, C. E. Svensson, E. Timakova, R. Wadsworth, J. Williams, M. S. C. Winokan, C. Y. Wu, T. Zidar, Coulomb excitation of 80,82 Kr and a change in structure approaching n=z=40, Phys. Rev. C 104 (2021) 044313.
- [17] GRIFFIN Collaboration, GRSISort: v4.0.0.3, https://doi.org/10.5281/zenodo.6330017, 2022.
- [18] R. Brun, F. Rademakers, ROOT An object oriented data analysis framework, Nuclear Instruments and Methods in Physics Research Section A: Accelerators, Spectrometers, Detectors and Associated Equipment 389 (1997) 81–86. New Computing Techniques in Physics Research V.
- [19] T. Czosnyka, D. Cline, C.-Y. Wu, Bull. Am. Phys. Soc. (1983).
- [20] J. F. Ziegler, M. Ziegler, J. Biersack, SRIM The stopping and range of ions in matter (2010), Nuclear Instruments and Methods in Physics Research Section B: Beam Interactions with Materials and Atoms 268 (2010) 1818–1823. 19th International Conference on Ion Beam Analysis.
- [21] J. Henderson, GOSIAFitter, 2023.
- [22] B. Singh, Nuclear data sheets for a = 80, Nuclear Data Sheets 105 (2005) 223-418.
- [23] W. Alford, R. Anderson, P. Batay-Csorba, R. Emigh, D. Lind, P. Smith, C. Zafiratos, A study of the (³He, n) reaction on isotopes of krypton, Nuclear Physics A 330 (1979) 77–90.
- [24] A. Giannatiempo, A. Nannini, A. Perego, P. Sona, M. J. G. Borge, O. Tengblad, Decay properties of the 0_2^+ state and spin-parity assignments in 78 Kr, Phys. Rev. C 52 (1995) 2444–2447.
- [25] A. Giannatiempo, A. Nannini, A. Passeri, A. Perego, P. Sona, Electric monopole transitions in ⁷⁶Se, Zeitschrift für Physik A Atomic Nuclei 325 (1986) 157–161.
- [26] K. Wrzosek-Lipska, K. Rezynkina, N. Bree, M. Zielińska, L. P. Gaffney, A. Petts, A. Andreyev, B. Bastin, M. Bender, A. Blazhev, B. Bruyneel, P. A. Butler, M. P. Carpenter, J. Cederkäll, E. Clément, T. E. Cocolios, A. N. Deacon, J. Diriken, A. Ekström, C. Fitzpatrick, L. M. Fraile, C. Fransen, S. J. Freeman, J. E. García-Ramos, K. Geibel, R. Gernhäuser, T. Grahn, M. Guttormsen, B. Hadinia, K. Hadyńska-Klęk, M. Hass, P. H. Heenen, R. D. Herzberg, H. Hess, K. Heyde, M. Huyse, O. Ivanov, D. G. Jenkins, R. Julin, N. Kesteloot, T. Kröll, R. Krücken, A. C. Larsen, R. Lutter, P. Marley, P. J. Napiorkowski, R. Orlandi, R. D. Page, J. Pakarinen, N. Patronis, P. J. Peura, E. Piselli, L. Próchniak, P. Rahkila, E. Rapisarda, P. Reiter, A. P. Robinson, M. Scheck, S. Siem, K. Singh Chakkal, J. F. Smith, J. Srebrny, I. Stefanescu, G. M. Tveten, P. Van Duppen, J. Van de Walle, D. Voulot, N. Warr, A. Wiens, J. L. Wood, Electromagnetic properties of low-lying states in neutron-deficient Hg isotopes: Coulomb excitation of ¹⁸²Hg, ¹⁸⁴Hg, ¹⁸⁶Hg and ¹⁸⁸Hg, The European Physical

- Journal A 55 (2019) 130.
- [27] N. Kesteloot, B. Bastin, L. P. Gaffney, K. Wrzosek-Lipska, K. Auranen, C. Bauer, M. Bender, V. Bildstein, A. Blazhev, S. Bönig, N. Bree, E. Clément, T. E. Cocolios, A. Damyanova, I. Darby, H. De Witte, D. Di Julio, J. Diriken, C. Fransen, J. E. García-Ramos, R. Gernhäuser, T. Grahn, P.-H. Heenen, H. Hess, K. Heyde, M. Huyse, J. Iwanicki, U. Jakobsson, J. Konki, T. Kröll, B. Laurent, N. Lecesne, R. Lutter, J. Pakarinen, P. Peura, E. Piselli, L. Próchniak, P. Rahkila, E. Rapisarda, P. Reiter, M. Scheck, M. Seidlitz, M. Sferrazza, B. Siebeck, M. Sjodin, H. Tornqvist, E. Traykov, J. Van De Walle, P. Van Duppen, M. Vermeulen, D. Voulot, N. Warr, F. Wenander, K. Wimmer, M. Zielińska, Deformation and mixing of coexisting shapes in neutron-deficient polonium isotopes, Phys. Rev. C 92 (2015) 054301.
- [28] E. Clément, M. Zielińska, S. Péru, H. Goutte, S. Hilaire, A. Görgen, W. Korten, D. T. Doherty, B. Bastin, C. Bauer, A. Blazhev, N. Bree, B. Bruyneel, P. A. Butler, J. Butterworth, J. Cederkäll, P. Delahaye, A. Dijon, A. Ekström, C. Fitzpatrick, C. Fransen, G. Georgiev, R. Gernhäuser, H. Hess, J. Iwanicki, D. G. Jenkins, A. C. Larsen, J. Ljungvall, R. Lutter, P. Marley, K. Moschner, P. J. Napiorkowski, J. Pakarinen, A. Petts, P. Reiter, T. Renstrøm, M. Seidlitz, B. Siebeck, S. Siem, C. Sotty, J. Srebrny, I. Stefanescu, G. M. Tveten, J. Van de Walle, M. Vermeulen, D. Voulot, N. Warr, F. Wenander, A. Wiens, H. De Witte, K. Wrzosek-Lipska, Low-energy Coulomb excitation of ^{96,98}Sr beams, Phys. Rev. C 94 (2016) 054326.
- [29] J. Heese, K. P. Lieb, S. Ulbig, B. Wörmann, J. Billowes, A. A. Chishti, W. Gelletly, C. J. Lister, B. J. Varley, Electromagnetic transition strengths between high spin states in ⁷⁹Sr and ⁸⁰Sr, Phys. Rev. C 41 (1990) 603–617.
- [30] D. Rhodes, B. A. Brown, J. Henderson, A. Gade, J. Ash, P. C. Bender, R. Elder, B. Elman, M. Grinder, M. Hjorth-Jensen, H. Iwasaki, B. Longfellow, T. Mijatović, M. Spieker, D. Weisshaar, C. Y. Wu, Exploring the role of high-j configurations in collective observables through the coulomb excitation of ¹⁰⁶Cd, Phys. Rev. C 103 (2021) L051301.
- [31] J. Henderson, Convergence of electric quadrupole rotational invariants from the nuclear shell model, Phys. Rev. C 102 (2020) 054306.
- [32] W. Satula, D. Dean, J. Gary, S. Mizutori, W. Nazarewicz, On the origin of the wigner energy, Physics Letters B 407 (1997) 103–109.
- [33] F. Becker, A. Petrovici, J. Iwanicki, N. Amzal, W. Korten, K. Hauschild, A. Hurstel, C. Theisen, P. Butler, R. Cunningham, T. Czosnyka, G. de France, J. Gerl, P. Greenlees, K. Helariutta, R.-D. Herzberg, P. Jones, R. Julin, S. Juutinen, H. Kankaanpää, M. Muikku, P. Nieminen, O. Radu, P. Rahkila, C. Schlegel, Coulomb excitation of ⁷⁸Kr, Nuclear Physics A 770 (2006) 107 125.
- [34] K. Kumar, Intrinsic Quadrupole Moments and Shapes of Nuclear Ground States and Excited States, Phys. Rev. Lett. 28 (1972) 249–253.
- [35] D. Cline, Nuclear Shapes Studied by Coulomb Excitation, Annual Review of Nuclear and Particle Science 36 (1986) 683–716.